Virus-Infected Alveolar Epithelial Cells Direct Neutrophil Chemotaxis and Inhibit Their Apoptosis

Joanna P. Rzepka[1], Anoria K. Haick[1], and Tanya A. Miura[1]

[1]Department of Biological Sciences, University of Idaho, Moscow, Idaho

The alveolar epithelium is a critical target for pulmonary viruses and can produce proinflammatory cytokines and chemokines upon viral infection. However, the molecular interactions between virus-infected alveolar epithelial cells and inflammatory cells, including polymorphonuclear leukocytes (PMNs), have not been thoroughly characterized. Rat coronavirus (RCoV) is used as a model to study the immune response to viral infection in the lung of the natural host. We have developed an *in vitro* model to characterize the response of PMNs to RCoV-infected type I-like alveolar epithelial (AT1) cells, the primary target for RCoV infection in the alveoli. Multiple CXC chemokines that signal through CXCR2 were required for PMN chemotaxis toward medium from RCoV-infected AT1-like cells (RCoV-AT1). Furthermore, RCoV-AT1 inhibited spontaneous PMN apoptosis, including activation of effector caspase 3 and initiator caspases 8 and 9. Use of a selective inhibitor of CXCR2, SB265610, demonstrated that CXCR2 signaling was required for RCoV-AT1–mediated inhibition of PMN apoptosis. These data suggest that CXC chemokines produced by RCoV-infected AT1-like cells inhibit PMN apoptosis during infection. These studies provide new insight into the molecular mechanisms whereby alveolar epithelial cells direct the functions of PMNs during viral infection of the lung.

Keywords: alveolar epithelial cells; neutrophils; rat coronavirus; CXC chemokines; CXCR2

CLINICAL RELEVANCE

Pulmonary viruses target alveolar epithelial cells, and neutrophilic inflammation is often associated with disease pathology. Using a rodent model of respiratory viral infection, this research identifies the underlying mechanisms whereby virus-infected alveolar epithelial cells direct neutrophil functions. When combined with *in vivo* studies, this knowledge contributes to the understanding of viral pathogenesis in the lung.

Numerous viruses infect the epithelial cells that line the respiratory tract, and increased pathogenesis is associated with the spread of viral infection to the alveoli. Viral antigens or nucleic acids have been found in type I (AT1) and/or type II (AT2) alveolar epithelial cells in autopsy material from fatal infections with severe acute respiratory syndrome–associated coronavirus, respiratory syncytial virus (RSV), and avian (H5N1) and 2009 pandemic (H1N1) influenza A viruses (1–4). These findings have been replicated in animal models that show a correlation between alveolar infection and disease severity (5, 6). Damage to the alveolar surface and respiratory distress during viral infections are often associated with the infiltration of inflammatory cells into the alveoli, yet these responses are necessary to mount effective antiviral immune responses that eliminate the infection. PMNs are recruited to the respiratory tract early during viral infections and can contribute to effective immune responses but also can enhance pathology (7, 8). Despite their importance in viral pathogenesis, little is known about the interactions between alveolar epithelial cells and the PMNs that contribute to inflammatory responses to viral infection.

In addition to providing a barrier between inhaled air and the host, the epithelium of the respiratory tract actively participates in host defense. For example, Stat1 is required by airway epithelial cells, but not hematopoietic cells, to control Sendai virus infection in mice (9). Although several studies have characterized proinflammatory responses to viral infection of epithelial cells from the conducting airways or immortalized cell lines, fewer studies have focused on the physiologically relevant cells of the alveoli (10). AT2 cells can be isolated from human or rodent lungs and cultured to maintain a highly differentiated AT2 cell phenotype or transdifferentiate into an AT1-like cell phenotype (11, 12). Due to the difficulty of isolating primary AT1 cells, *in vitro* transdifferentiated AT1-like cells are commonly used to study AT1 cell functions *in vitro*. The AT1-like phenotype is characterized by a loss of AT2 and a gain of AT1 cell markers (12). Highly differentiated cultures of human AT2 and AT1-like cells express proinflammatory cytokines and chemokines upon infection with influenza A virus (13, 14). Furthermore, the expression of high levels of proinflammatory cytokines by alveolar epithelial cells correlates with the relative virulence of influenza virus strains (14). Because the alveolar epithelium is an important target for viral infection and expresses proinflammatory cytokines and chemokines in response to infection, we propose that these cells are critical for the initiation and regulation of immune responses in the lung.

Rat coronavirus (RCoV) infects and causes acute inflammatory disease in the respiratory tract of rats, providing a model to study respiratory viral pathogenesis in the natural host of the virus (15). Adult rats infected intratracheally with RCoV have increased levels of CXC chemokines in bronchoalveolar lavage fluid, which is correlated with the recruitment of PMNs to the airways (15). Viral antigen is predominantly found in AT1 cells within the alveoli of RCoV-infected rats (15). RCoV induces expression of proinflammatory cytokines and chemokines by rat AT1-like cells *in vitro* (16), suggesting that AT1 cells may play a critical role in the inflammatory response to RCoV infection. To study the interactions between the alveolar epithelium and PMNs during coronaviral infection, supernatant medium from RCoV-infected AT1-like cells was tested for the ability to promote chemotaxis and alter PMN apoptosis. Furthermore,

(*Received in original form July 1, 2007 and in final form January 27, 2012*)

This work was supported by the INBRE Program, NIH Grant Nos. P20 RR016454 (National Center for Research Resources) and P20 GM103408 (National Institute of General Medical Sciences); and NIH Grants P20 RR015587 (National Center for Research Resources) and U54 AI081680 (National Institute of Allergy and Infectious Diseases).

Correspondence and requests for reprints should be addressed to Tanya A. Miura, Ph.D., Department of Biological Sciences, University of Idaho, PO Box 443051, Moscow, ID 83844-3051. E-mail: tmiura@uidaho.edu

This article has an online supplement, which is accessible from this issue's table of contents at www.atsjournals.org

Am J Respir Cell Mol Biol Vol 46, Iss. 6, pp 833–841, Jun 2012

Originally Published in Press as DOI: 10.1165/rcmb.2011-0230OC on February 2, 2012
Internet address: www.atsjournals.org

the molecular mechanisms that mediate these functions were defined. Further studies are needed to determine the *in vivo* relevance of these interactions to viral pathogenesis in the lung.

MATERIALS AND METHODS

Cells and Virus

Animal protocols were approved by the University of Idaho Animal Care and Use Committee according to the National Research Council Guide for the Care and Use of Laboratory Animals. AT2 cells were isolated from 6- to 10-week-old Simonsen Albino rats (Simonsen Laboratories, Gilroy, CA) and transdifferentiated to an AT1-like phenotype (16). RCoV strain sialodacryoadenitis virus, obtained from Dr. Kathryn Holmes (University of Colorado Denver, Aurora, CO), was purified by sucrose density gradient centrifugation and stored in TMS buffer as described (16). AT1-like cells were inoculated with RCoV or TMS (mock) diluted in Dulbecco's modified Eagle medium. After infection, cells were supplemented with RPMI/10% FBS/2% PSF (RPMI). Viral infection was confirmed by immunofluorescent detection of viral nucleocapsid antigen (16), and supernatant medium was harvested 24 hours after viral inoculation for chemotaxis and apoptosis assays.

PMNs

Rats were killed with an overdose of sodium pentobarbital, and blood was collected into heparin (500 U). Erythrocytes were removed by dextran sedimentation, and granulocytes were separated by centrifugation over Histopaque 1083. Residual erythrocytes were lysed, and granulocytes were resuspended in endotoxin-free HBSS/1% BSA and kept on ice. To isolate PMNs from bone marrow, femurs and tibias were flushed with HBSS/1% BSA, and erythrocytes were lysed before granulocyte separation using Ficoll. All preparations consisted of approximately 95% PMNs, with less than 5% eosinophils, lymphocytes, and monocytes, based on differential cell staining.

Chemotaxis Assays

Supernatant media from RCoV-infected (RCoV-AT1), mock-inoculated (mock-AT1), and uninfected (RPMI-AT1) AT1-like cells were tested in chemotaxis assays using ChemoTx chambers with a 3-μm pore filter (NeuroProbe, Gaithersburg, MD) (17). Migration of 3×10^4 calcein-AM–labeled PMNs to the lower chamber was quantified using a FLUOstar Optima fluorescence plate reader (BMG LabTech, San Francisco, CA), in comparison to a standard curve (*see* Figure E1 in the online supplement). Where indicated, PMNs were treated with SB265610 (100 nM) or vehicle (DMSO), or neutralizing antibodies against CXC chemokines were added to the medium in the lower chamber before chemotaxis assay.

PMN Apoptosis

PMN apoptosis was induced by cycloheximide (Cx) (100 ng/ml), hrTNF-α (0.1 mg/ml), or exposure to 15,000 μJ UV irradiation for 15 minutes in a StrataLinker UV Crosslinker (Stratagene, Santa Clara, CA). SB265610 (100 nM) was added to PMNs where indicated. Cells were stained with annexin V-FITC and propidium iodide and analyzed by flow cytometry using FACSAria and FACSDiva 6.0 software (BD Biosciences, San Jose, CA). The activity of caspases 2, 3, 8, or 9 was quantified using luminescent substrate assays (Caspase-Glo; Promega Corp., Madison, WI). Caspase 2 activity was measured in the presence of Ac-DEVD-CHO (1 mM) and MG132 (60 μM). Luminescence was measured using a FLUOstar Optima, and data analysis was performed using MARS software (BMG Labtech Inc.).

Statistical Analysis

Statistical analysis was performed using Prism 5.00 (GraphPad Software, San Diego, CA). *P* values were obtained using one-way ANOVA and Newman-Keuls multiple comparison test.

RESULTS

Rat PMNs Actively Migrate toward Medium from RCoV-Infected, but not Mock-Inoculated, AT1-Like Cells

Viral antigen is predominantly found in AT1 cells in the alveoli of RCoV-infected rats, and PMNs are present at high levels in bronchoalveolar lavage fluid early during infection (15). We propose that RCoV-infected AT1 cells recruit PMNs to the lung during infection. An *in vitro* chemotaxis assay was used to test whether rat bone marrow–derived PMNs actively migrate toward supernatant medium harvested from AT1-like cells 24 hours after infection by RCoV. Fluorescently labeled PMNs were placed in the upper chamber of a chemotaxis plate, and medium to be analyzed for chemoattractant ability was placed in the lower chamber. Fluorescence intensity was measured in the lower chamber to quantify PMN migration through the 0.3-μm filter separating the two chambers. A standard curve was generated to estimate cell number based on fluorescence intensity (Figure E1). Chemotaxis of PMNs toward the bacterial tripeptide FMLP was considered to represent 100% chemotaxis. PMNs had approximately 20% chemotaxis toward RPMI medium alone. PMNs underwent significant chemotaxis toward medium from RCoV-infected AT1-like cells (RCoV-AT1) but not to medium from mock-inoculated (mock-AT1) or noninfected (RPMI-AT1) cells (Figure 1A). The medium from RCoV-infected cells contains viral particles; therefore, we quantified PMN chemotaxis toward

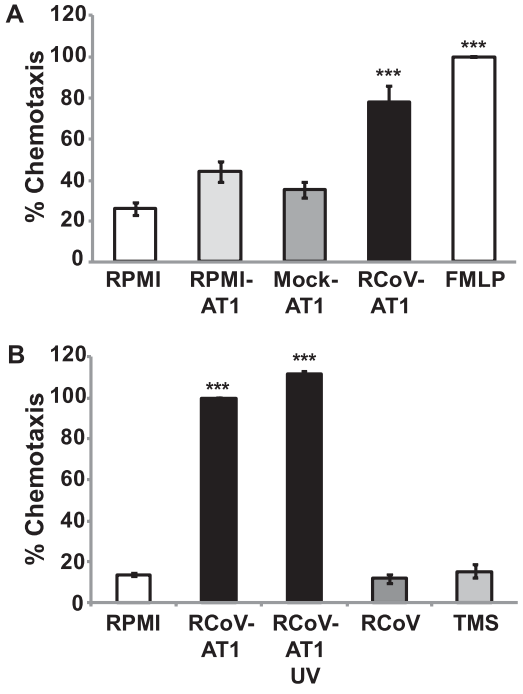

Figure 1. Chemotaxis of rat polymorphonuclear leukocytes (PMNs) toward medium from rat coronavirus (RCoV)-infected AT1-like cells. Rat PMNs were isolated from bone marrow and stained with calcein-AM, and the chemotaxis of 3×10^4 PMNs was quantified by fluorescence intensity in a micro-chemotaxis plate. (*A*) RPMI, medium from uninfected (RPMI-AT1 and Mock-AT1) or RCoV-infected (RCoV-AT1) AT1-like cells, or FMLP were placed in the lower chamber of the chemotaxis plate. Fluorescence intensity data were normalized to FMLP. (*B*) RCoV-AT1, UV-irradiated RCoV-AT1, purified virus, and virus storage buffer (TMS) were placed in the lower chamber of the chemotaxis plate. Fluorescence intensity data were normalized to RCoV-AT1. Data are means ± SEM from at least three independent experiments with triplicate samples per experiment. Statistical significance versus RPMI: ***$P < 0.001$.

purified virus. In comparison to chemotaxis toward RCoV-AT1, purified RCoV or viral storage buffer (TMS) did not induce PMN chemotaxis (Figure 1B). Finally, RCoV-AT1 was UV irradiated, which inactivates viral infectivity, before incubation with PMNs. UV irradiation of RCoV-AT1 did not reduce PMN chemotaxis (Figure 1B). Taken together, these data indicate that PMNs actively migrate toward a soluble factor secreted by RCoV-infected AT1-like cells and not to virus particles.

Signaling by CXCR2 Is Required for PMN Chemotaxis toward RCoV-AT1

To further investigate the mechanism whereby RCoV-AT1 medium induces PMN chemotaxis, we evaluated the role of CXCR2, which is the common receptor for rat CXC chemokines (18). Rat PMNs were incubated with an antagonist of CXCR2, SB265610, before exposure to RCoV-AT1 in the chemotaxis assay (19). PMNs treated with SB265610 had significantly reduced chemotaxis toward RCoV-AT1 (Figure 2). However, SB265610 did not reduce chemotaxis of PMN to the same level as toward RPMI alone. Preincubation of PMNs with vehicle alone (DMSO) did not alter migration toward RCoV-AT1. Thus, inhibition of CXCR2 signaling significantly decreased PMN chemotaxis toward RCoV-AT1, although not completely to background levels.

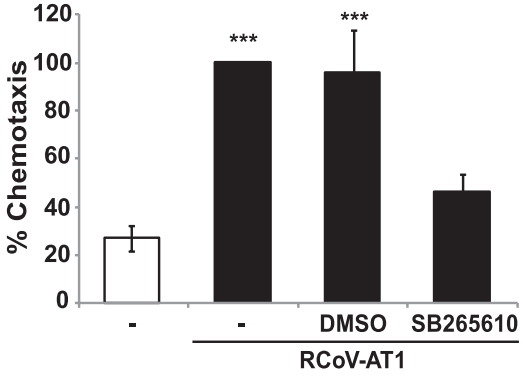

Figure 2. The role of CXCR2 signaling in PMN chemotaxis toward RCoV-AT1. Rat PMNs were isolated from bone marrow and stained with calcein-AM, and the chemotaxis of 3×10^4 PMNs was quantified by fluorescence intensity in a micro-chemotaxis plate toward RPMI or RCoV-AT1 in the presence or absence of CXCR2 inhibitor (SB265610) or vehicle (DMSO). Fluorescence intensity data were normalized to RCoV-AT1. Data shown are the mean values ± SEM from three independent experiments with triplicate samples per experiment. Statistical significance versus RCoV-AT1 with SB265610: $***P < 0.001$.

Multiple CXC Chemokines Produced by RCoV-Infected AT1-Like Cells Promote Chemotaxis of Rat PMNs

Because multiple rat CXC chemokines are known ligands of CXCR2, we tested their individual roles in PMN chemotaxis to RCoV-AT1 medium. Chemotaxis was not affected by the addition of neutralizing antibody to any one of the CXC chemokines alone (Figure 3A). However, when all four ELR+ CXC chemokines (CXCL1, CXCL2, CXCL3, and CXCL5) were neutralized, PMN chemotaxis decreased by more than 60% (Figure 3B). Similar to the CXCR2 inhibitor, neutralization of the four CXC chemokines did not completely block PMN chemotaxis toward RCoV-AT1. If a combination of three antibodies included anti-CXCL1 and anti-CXCL3, PMN chemotaxis was inhibited to a similar level as with all four antibodies. The use of neutralizing antibodies to CXCL1 and CXCL3 together inhibited PMN chemotaxis by approximately 40%, which was statistically significant but not as effective as neutralization of all four CXC chemokines. Isotype control antibodies did not affect PMN chemotaxis toward RCoV-AT1 (Figure 3A). The specificity of each neutralizing antibody was tested against recombinant CXC chemokines (Figure E2). These experiments confirmed that each antibody neutralized the chemoattractant activity of its specific CXC protein. The antibodies also had various levels of cross-reactivity to the other CXC chemokines. Anti-CXCL1 completely blocked chemotaxis toward rCXCL1 and partially inhibited chemotaxis toward rCXCL3. Anti-CXCL3 neutralized the function of rCXCL2 and rCXCL3 but did not significantly reduce chemotaxis toward rCXCL1. Anti-CXCL5 only inhibited PMN chemotaxis toward rCXCL5; however, chemotaxis of PMNs to rCXCL5 was much lower than toward the other recombinant proteins. To determine whether the concentrations of individual CXC chemokines in RCoV-AT1 correlated with the results from the neutralization experiments, CXC chemokines were quantified in RCoV-AT1 medium at 24, 48, and 72 hours after infection (Figure 3C). All of the CXC chemokines tested were induced by RCoV in AT1-like cells by 24 hours, which was the time point used for the chemotaxis experiments. CXCL1 and CXCL3 were the most abundant CXC chemokines in RCoV-AT1 medium through the time course of RCoV infection. The concentration of CXCL5 was similar to CXCL1 at 24 hours but did not increase comparably over time. CXCL2 was secreted at relatively low concentrations at all time points. These data suggest that multiple CXC chemokines signaling through CXCR2 contribute to PMN chemotaxis toward RCoV-AT1. CXCL1 and CXCL3 seem to be the most critical for PMN chemotaxis and, along with CXCL5, are the most abundant CXC chemokines in RCoV-AT1 medium used for the chemotaxis experiments.

PMN chemotaxis toward RCoV-AT1 was significantly, but not completely, inhibited by CXCR2 inhibitor (Figure 2) or neutralizing antibodies to all four CXC chemokines (Figure 3B). We previously showed that AT1 cells secrete multiple cytokines and chemokines upon infection with RCoV (16). It is possible that other factors, in addition to CXC chemokines, contribute to PMN chemotaxis toward RCoV-AT1. In addition, CXC chemokines form biologically active homodimers and heterodimers (20–22). It is not known whether neutralizing antibodies effectively inhibit chemotaxis toward CXC chemokines when present in mixed solutions of monomers, homodimers, and heterodimers. To further examine the molecular basis of PMN chemotaxis toward RCoV-AT1, recombinant CXC chemokines were combined at concentrations equivalent to those in RCoV-AT1 and analyzed in a PMN chemotaxis assay. PMN chemotaxis toward the mixture of recombinant CXC chemokines was approximately 20% lower than toward RCoV-AT1 (Figure 3D), which contains comparable concentrations of CXC chemokines. In contrast to the results with RCoV-AT1, PMN chemotaxis toward the recombinant CXC chemokines in combination was completely inhibited by the four neutralizing antibodies (Figure 3D). These data indicate that, under our assay conditions, interactions between multiple CXC chemokines do not interfere with neutralization of their PMN chemoattractant functions by these antibodies. Therefore, the incomplete neutralization of PMN chemotaxis toward RCoV-AT1 using anti-CXC antibodies is likely due to additional factors in RCoV-AT1 that promote PMN chemotaxis.

Spontaneous Apoptosis of PMNs Is Inhibited by Medium from RCoV-Infected AT1-Like Cells

PMNs contribute to tissue damage during respiratory viral infections due to the release of cytotoxic mediators. Rapid spontaneous apoptosis of PMNs limits damage and is critical for resolution of neutrophilic inflammation. To identify interactions between the virus-infected alveolar epithelium and PMNs that may affect

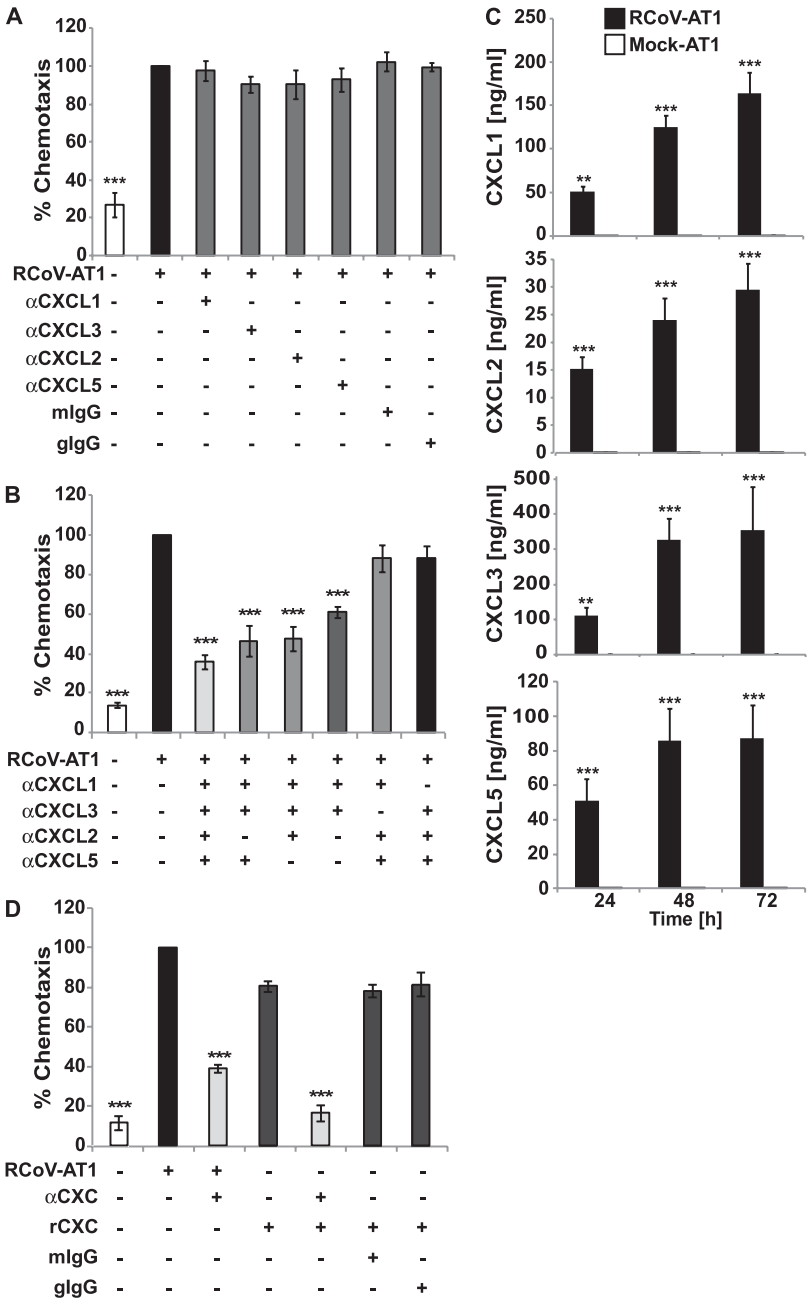

Figure 3. Chemotaxis of PMNs toward RCoV-AT1 in the presence of neutralizing antibodies to CXC chemokines. Rat PMNs were isolated from bone marrow and stained with calcein-AM, and the chemotaxis of 3×10^4 PMNs toward RCoV-AT1 was quantified by fluorescence intensity in a micro-chemotaxis plate. RCoV-AT1 was incubated with the indicated antibodies before chemotaxis assay. Fluorescence intensity data were normalized to RCoV-AT1. (*A*) The ability of individual αCXC antibodies to neutralize chemotaxis toward RCoV-AT1 was evaluated. Mouse IgG (mIgG) was used as an isotype control for αCXCL2, -3, and -5 and goat IgG (gIgG) was used as an isotype control for αCXCL1. (*B*) Multiple antibodies were evaluated in combination. ***Statistical significance versus RCoV-AT1 ($P < 0.001$). (*C*) The concentrations of CXC chemokines in RCoV-AT1 compared with mock-AT1 at 24, 48, and 72 hours after inoculation were quantified by ELISA. Statistical significance versus mock-AT1: **$P < 0.01$, ***$P < 0.001$. (*D*) Chemotaxis of PMNs toward recombinant CXC chemokines (rCXC) at equivalent concentrations as in RCoV-AT1 was quantified with or without the addition of neutralizing antibodies to the four chemokines (αCXC). ***Statistical significance versus RCoV-AT1 ($P < 0.001$). Data shown are means ± SEM from at least three independent experiments with triplicate samples per experiment.

PMN apoptosis, we analyzed the impact of RCoV-AT1 medium on spontaneous PMN apoptosis *in vitro*. PMNs isolated from rat blood were incubated in RCoV-AT1 or mock-AT1 medium, and apoptosis was analyzed over time. As expected, the proportion of PMNs that bound annexin V increased during incubation in RPMI-AT1 (from 25.6 ± 5.2% at 0 h to 79.5 ± 4.6% at 48 h) (Figure 4A). This rate of apoptosis is similar to the spontaneous apoptosis of human PMNs incubated *in vitro* reported by others (23, 24). Incubation of PMNs in RCoV-AT1 resulted in a significant inhibition of apoptosis compared with PMNs incubated in mock-AT1 or RPMI-AT1 at the 24- and 48-hour time points. There was no significant difference in annexin V binding to PMNs incubated in mock-AT1 or RPMI-AT1 compared with RPMI alone (data not shown).

Effector caspase 3 is activated during spontaneous apoptosis of human PMNs, and inhibition of caspase 3 reduces PMN apoptosis (24, 25). Therefore, we analyzed the activity of caspase 3 in PMNs incubated in RPMI or RCoV-AT1 using the Caspase-Glo 3/7 Assay (Promega Corp.), which does not distinguish between caspases 3 and 7. As expected, caspase 3/7 was activated in PMNs incubated in RPMI. Incubation of PMNs in RCoV-AT1 significantly inhibited activation of caspase 3/7 at 6 hours compared with incubation in RPMI (Figure 4B). Caspase 3 can be activated by initiator caspase 8, which is activated by death receptor adapter proteins, or caspase 9, which is activated by the apoptosome after mitochondrial membrane depolarization. Both caspase 8 and 9 are activated during spontaneous apoptosis of PMNs (25). As expected, caspases 8 and 9 had significantly increased activity in PMNs by 4 hours after isolation (data not shown). Incubation of PMNs in RCoV-AT1 inhibited the enzymatic activity of caspases 8 and 9 at 4 hours (Figure 4B). This suggests that RCoV-AT1 inhibits an early step in caspase 8– and caspase 9–dependent pathways of PMN apoptosis.

Although the role of caspase 2 in the spontaneous apoptosis program of PMNs has not been defined, caspase 2 induces apoptotic signaling upstream of the mitochondrium (26). Caspase 2 is

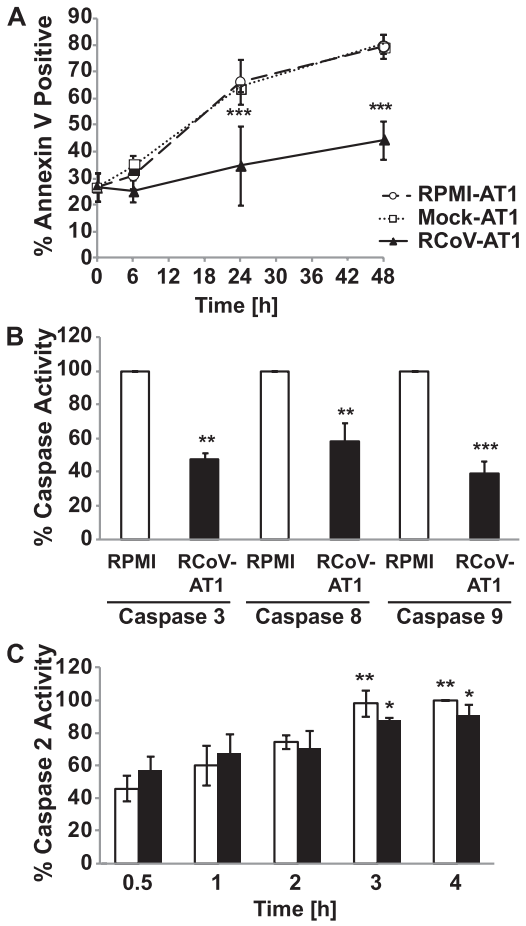

Figure 4. RCoV-AT1–mediated inhibition of spontaneous PMN apoptosis. (*A*) PMNs were isolated from rat blood and incubated with supernatant medium from noninfected (RPMI-AT1), mock-infected (Mock-AT1), or RCoV-infected (RCoV-AT1) AT1-like cells and annexin V-FITC binding was analyzed by flow cytometry. (*B*) The activities of effector caspase 3 (after 6-h incubation), initiator caspases 8 and 9 (after 4-h incubation), and (*C*) caspase 2 (at indicated times) were quantified in PMNs incubated in RPMI or RCoV-AT1 using luminescent substrate assays. Luminescence intensities were normalized to PMNs incubated in RPMI. Data shown are means ± SEM from at least three independent experiments. Statistical significance versus (*A*) RPMI-AT1, (*B*) RPMI, or (*C*) RPMI at 0.5 h: $*P < 0.05$, $**P < 0.01$, and $***P < 0.001$.

also activated by death domain–containing receptors, but, unlike caspase 8, caspase 2 activation is independent of Fas-Associated protein with Death Domain (27). Caspase 2 activity during spontaneous apoptosis of PMN was quantified and compared with PMN incubated in RCoV-AT1. Caspase 2 activity in PMNs increased significantly during 4 hours of culture *in vitro* (Figure 4C). However, caspase 2 activation was not affected by incubation of PMNs in RCoV-AT1, suggesting that inhibition of caspase 2 activation is not required for RCoV-AT1–mediated inhibition of PMN apoptosis. In summary, medium from RCoV-infected, but not mock-inoculated, AT1-like cells inhibited spontaneous apoptosis of PMNs *in vitro*, including activation of caspases 3/7, 8, and 9 but not caspase 2.

Soluble Factors Secreted by RCoV-Infected AT1-Like Cells, but Not Viral Particles, Inhibit PMN Apoptosis

RSV directly inhibits PMN apoptosis, which is dependent upon endosomal uptake of the virus (28). Therefore, we determined whether viral particles in RCoV-AT1 medium directly inhibit spontaneous apoptosis of rat PMNs. PMNs were incubated in RPMI containing sucrose gradient–purified RCoV at a concentration approximately equal to that in RCoV-AT1 or viral storage buffer (TMS), and apoptosis was analyzed by annexin V binding and flow cytometry. Spontaneous apoptosis was not altered by incubation of PMNs with purified virus or TMS compared with incubation in RPMI alone (Figure 5A). To confirm that infectious virus particles are not required to inhibit PMN apoptosis, RCoV-AT1 was UV irradiated before incubation with PMNs. UV irradiation has been shown to completely inactivate RCoV (16). However, irradiation of RCoV-AT1 did not affect its ability to inhibit spontaneous apoptosis of PMNs (Figure 5A). These data together suggest that a soluble factor(s) secreted by RCoV-infected AT1-like cells, rather than infectious virus particles alone, inhibits PMN apoptosis.

Signaling through CXCR2 Is Required for RCoV-AT1–Mediated Inhibition of PMN Apoptosis

CXC chemokines, including human IL-8 and GRO-α and rat CXCL1, inhibit PMN apoptosis (19, 23, 29, 30). Rat CXC chemokines are ligands for CXCR2 (18). Therefore, we inhibited CXCR2 signaling with SB265610 to analyze whether CXCR2 signaling was required for RCoV-AT1–mediated suppression of PMN apoptosis. Rat PMNs were incubated in RPMI or RCoV-AT1 with or without SB265610, and apoptosis was analyzed by annexin V binding and caspase 3 activity. SB265610 did not alter spontaneous apoptosis of PMNs, as shown by incubation in RPMI (Figures 5B and 5C). However, the inhibition of apoptosis by RCoV-AT1 was reversed to the level of spontaneous apoptosis by the addition of SB265610. The addition of DMSO did not alter PMN apoptosis (data not shown). Taken together, these data demonstrate that RCoV-AT1 inhibits PMN apoptosis by signaling through CXCR2, suggesting that one or more CXC chemokines expressed by RCoV-infected AT1-like cells inhibit PMN apoptosis.

PMN Apoptosis Induced by TNF-α Is Inhibited by RCoV-AT1

RCoV-AT1 inhibited activation of caspases 8 and 9 (Figure 4B), which initiate apoptosis triggered by extrinsic and intrinsic signals, respectively. To determine whether RCoV-AT1 could inhibit apoptosis induced by extrinsic and intrinsic signals, PMNs were incubated in RCoV-AT1 or RPMI in the presence of TNF-α or Cx for 6 hours, or PMNs were UV irradiated and then incubated for 6 hours with RCoV-AT1 or RPMI. TNF-α, Cx, and UV irradiation all induced PMN apoptosis as compared with PMN incubated in RPMI (Figure 6A). RCoV-AT1 had no significant effect on UV- or Cx-induced apoptosis. In contrast, incubation in RCoV-AT1 dramatically decreased TNF-α–induced PMN apoptosis, as demonstrated by annexin V binding and caspase 3 activation (Figures 6A and 6B). Mock-AT1 had no effect on PMN apoptosis induced by TNF-α, Cx, or UV light (data not shown). In summary, medium from RCoV-infected AT1-like cells inhibited spontaneous and TNF-α–induced PMN apoptosis, suggesting inhibition of a pathway shared by both apoptotic programs.

DISCUSSION

The alveolar epithelium is an important target for viruses that infect the lung (1–4). Communication between virus-infected epithelial cells and PMNs initiates and regulates the subsequent response in the lung. The purpose of this study was to characterize the response of PMNs to virus-infected alveolar epithelial cells. RCoV is a respiratory pathogen of rats that predominantly infects AT1 cells in the alveoli and induces a robust influx of PMNs

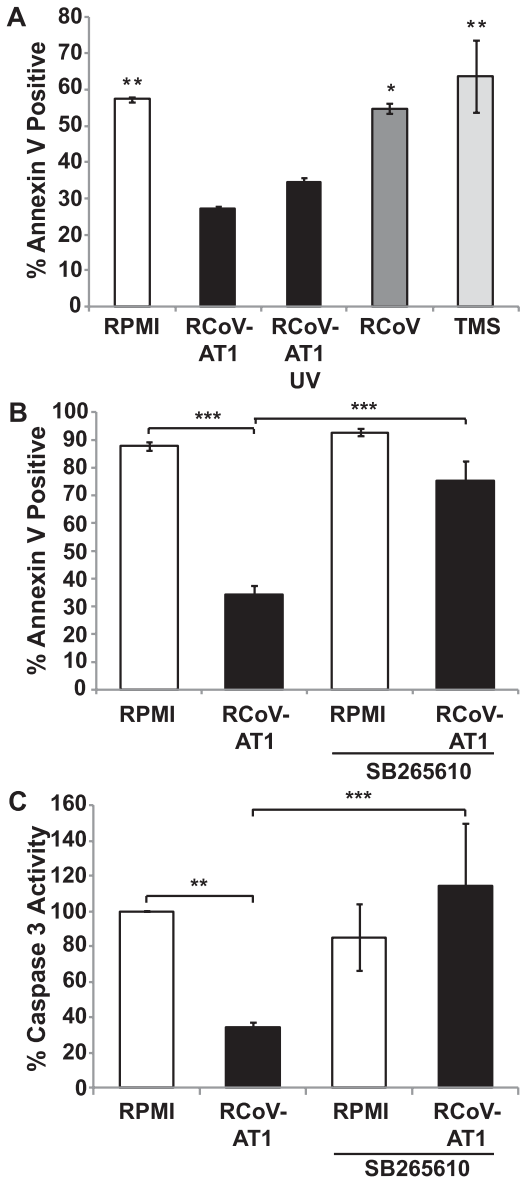

Figure 5. The role of viral particles and CXCR2 signaling in RCoV-AT1–mediated inhibition of spontaneous PMN apoptosis. PMNs were isolated from rat blood. (*A*) Apoptosis of PMNs incubated with UV-irradiated RCoV-AT1 or purified RCoV or virus storage buffer (TMS) for 24 hours was analyzed by annexin V-FITC binding and flow cytometry. Apoptosis of PMNs incubated with RCoV-AT1 with or without CXCR2 inhibitor (SB265610) was analyzed by (*B*) annexin V-FITC binding and (*C*) caspase 3 activity using a luminescent substrate assay. Luminescence data were normalized to PMNs incubated in RPMI. Data shown are means ± SEM from at least three independent experiments. Statistical significance versus RCoV-AT1: $*P < 0.05$, $**P < 0.01$, and $***P < 0.001$.

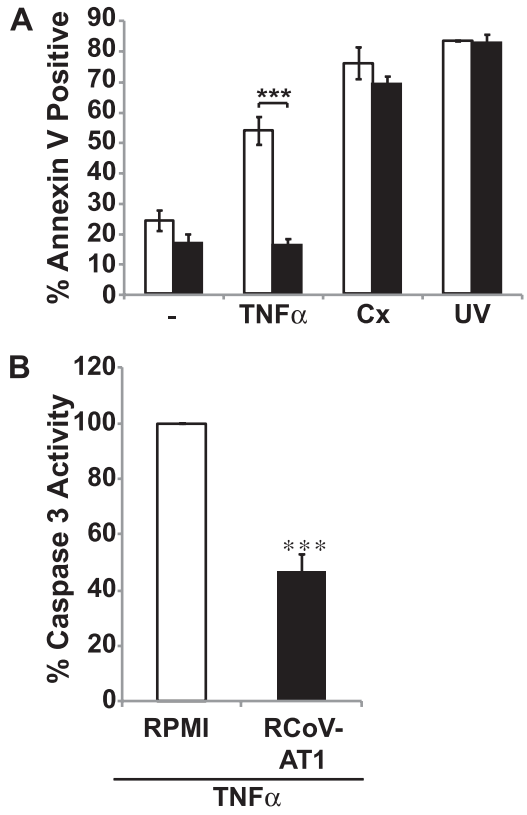

Figure 6. RCoV-AT1–mediated inhibition of induced PMN apoptosis. PMNs were isolated from rat blood and preexposed to UV irradiation or incubated with TNF-α or cycloheximide (Cx) in RPMI or RCoV-AT1. (*A*) Annexin V-FITC binding was quantified by flow cytometry, and (*B*) caspase 3 activity was analyzed by luminescent substrate assay. Luminescence data were normalized to PMNs incubated in RPMI with TNF-α. Data shown are the mean values ± SEM from at least three independent experiments. Statistical significance as indicated ($***P < 0.001$).

into the airways early during infection (15). We used *in vitro* transdifferentiated cultures of rat AT1-like cells as a well described model for AT1 cell functions (12). Medium from RCoV-AT1 was analyzed for the ability to induce chemotaxis and apoptosis of rat PMNs.

PMNs underwent active chemotaxis toward RCoV-AT1 but not mock-AT1 or purified virus, indicating that a soluble factor released by RCoV-infected AT1-like cells mediates chemotaxis. Furthermore, PMN chemotaxis toward RCoV-AT1 was reduced by a CXCR2 inhibitor and by neutralizing antibodies to multiple CXC chemokines. These experiments indicate that virus-infected alveolar epithelial cells can direct PMN chemotaxis through the production of CXC chemokines that signal through CXCR2 on PMNs. However, additional studies are needed to determine whether alveolar epithelial cells play a significant role in PMN recruitment *in vivo*. Although human PMNs express two functional receptors for ELR+ CXC chemokines (CXCR1 and CXCR2), rat PMNs only express functional CXCR2 (31). Furthermore, PMN chemotaxis toward RCoV-AT1 was significantly inhibited by SB265610, a nonpeptide inhibitor of CXCR2 that specifically inhibits chemotaxis of rat PMNs toward CXCL1 and CXCL2 *in vitro* and blocks recruitment of PMNs to the lungs of hyperoxia-exposed rats (19). CXCL1, CXCL2, CXCL3, and CXCL5 are ligands for rat CXCR2, yet they bind with different affinities and induce calcium mobilization at different levels (18, 31–33). Therefore, it was important to determine whether CXC chemokines have redundant functions in PMN chemotaxis. We show that neutralizing antibodies to individual CXC chemokines had no effect on PMN chemotaxis toward RCoV-AT1, suggesting redundant chemoattractant functions. Moreover, CXCL1 and CXCL3 were present in the highest concentrations in RCoV-AT1 medium, and neutralization of both of these chemokines simultaneously was required to reduce PMN chemotaxis. However, when all four CXC chemokines were neutralized simultaneously, PMN chemotaxis was not completely blocked compared with medium alone (Figure 3B). The neutralizing antibodies effectively blocked PMN chemotaxis toward their respective CXC chemokines (Figure E2). These results indicate that there may

be additional factors present in RCoV-AT1 that are promoting PMN chemotaxis when the CXC chemokines are neutralized.

Although the role of homo- and heterodimer formation in the biological activity of rat CXC chemokines has not been studied, multiple studies have evaluated the effect of dimerization on the activity of human CXCL8/IL-8. Although CXCL8 in solution fluctuates between monomeric and dimeric forms, fixed monomers and dimers that are unable to associate or dissociate, respectively, have been used to evaluate their chemoattractant activities. CXCL8 monomers exhibit increased, and dimers have decreased, CXCR1-dependent chemotaxis in comparison to wild-type CXCL8 (21). However, CXCR2-dependent chemotaxis does not differ in response to fixed monomeric or dimeric forms of CXCL8 (21). Furthermore, monomeric and dimeric forms of CXCL8 have biological activity *in vivo*, although the various forms have distinct roles in PMN recruitment (22). In addition to homodimers, CXCL8 forms heterodimers with a related CXC chemokine, PF4, which reduces the chemoattractant functions of CXCL8 (20). We show that neutralizing antibodies completely inhibited PMN chemotaxis toward the four recombinant CXC chemokines when combined at concentrations equivalent to that in RCoV-AT1 medium (Figure 3D). Thus, heterotypic interactions between CXC chemokines did not affect neutralization of their chemoattractant functions. Furthermore, upon neutralization of the CXC chemokines, additional chemoattractant activity remained (Figure 3B). These experiments, combined with the finding that CXCR2 inhibitor did not completely inhibit PMN chemotaxis (Figure 2), support the hypothesis that other factors, in addition to the ELR+ CXC chemokines, contribute to PMN chemotaxis toward RCoV-AT1.

Apoptosis of PMNs regulates their lifespan in circulation and promotes effective resolution of inflammatory responses. Inhibition of PMN apoptosis during infection can prolong their functional lifespan but can also delay resolution of inflammation. Because PMNs contain an arsenal of cytotoxic molecules, their death by apoptosis and rapid removal by phagocytic macrophages is critical for preventing untoward tissue damage. Apoptotic PMNs are phagocytosed by macrophages, thereby preventing the release of cytotoxic components, including reactive oxygen species and proteolytic enzymes that will damage the lung. In addition, phagocytosis of apoptotic PMNs has immunosuppressive effects on macrophages, which further down-regulates inflammatory responses. During inflammatory responses, the apoptotic program of PMNs can be delayed, thereby prolonging their functional lifespan but also contributing to pathology. Mimicking their short life span *in vivo*, PMNs undergo spontaneous apoptosis when incubated *in vitro* (23, 24). We observed that incubation of PMNs in RCoV-AT1 significantly inhibited their spontaneous apoptosis, including inhibition of initiator caspases 8 and 9 and effector caspase 3. We further showed that purified virus or UV inactivation of virus in RCoV-AT1 had no effect on PMN apoptosis. This is in contrast to other viruses that directly alter the apoptosis program of PMNs. Infectious and heat-inactivated RSV directly inhibits PMN apoptosis through activation of PI3K- and NF-κB–dependent prosurvival pathways (28). Furthermore, RSV induces expression of IL-6 by PMNs, which may provide autocrine regulation of PMN survival (28, 34, 35). In contrast to RSV, influenza A virus enhances PMN apoptosis *in vitro* (36). Our results demonstrate that purified RCoV, at a similar concentration as in RCoV-AT1 medium, does not directly affect spontaneous PMN apoptosis. Furthermore, we showed that incubation of PMNs in RCoV-AT1 with a CXCR2 inhibitor (SB265610) reversed apoptosis inhibition. This suggests that CXC chemokines that are induced by RCoV infection of AT1 cells are responsible for inhibiting PMN apoptosis. Multiple studies have demonstrated CXC chemokine–mediated inhibition of PMN apoptosis. Human PMNs have decreased spontaneous apoptosis in the presence of IL-8 and Gro-α (30, 37). Although IL-8 can bind to CXCR1 or CXCR2, a selective inhibitor of CXCR2 completely reverses the inhibitory effect of IL-8 on PMN apoptosis (37). Wang and colleagues showed that rat CXCL1 inhibits astrocyte apoptosis induced by ceramide through CXCR2 signaling (38). Apoptosis of rat PMNs is inhibited by culture in CXCL1, and this effect is reversed by pretreatment with SB265610, confirming that CXCR2 signaling is required for apoptosis inhibition (19, 23, 29).

In addition to CXC chemokines, PMN apoptosis is also inhibited by cytokines, including GM-CSF, G-CSF, IL-1β, IL-6, IFN-γ, TNF-α, and IL-15 (35, 39, 40). In contrast, other proinflammatory cytokines, such as TNF-α and IL-6, significantly induce PMN apoptosis (41–43). Separate studies have reported that TNF-α and IL-6 induce or inhibit PMN apoptosis depending on the cytokine concentration or activation state of the PMNs (44, 45). Additionally, Murray and colleagues demonstrated the importance of timing in TNF-α–induced PMN apoptosis (46). When apoptosis was evaluated at time points before 8 hours, TNF-α promoted PMN apoptosis. In contrast, when incubated over 18 hours, TNF-α decreased PMN apoptosis. In our study, TNF-α–induced apoptosis was evaluated after 6 hours of incubation of PMNs isolated from rat blood, and we confirmed by staining of activation markers that the PMNs were not activated by our isolation procedure (data not shown). Inhibition of CXCR2 signaling by SB265610 completely restored caspase 3 activity in PMNs incubated in RCoV-AT1, suggesting that CXC chemokines in RCoV-AT1 are sufficient to inhibit caspase 3 activity in PMNs. However, the percentage of PMNs that bound annexin V was not completely restored when SB265610 was used. Thus, we cannot rule out the possibility that cytokines, in addition to CXC chemokines, present in RCoV-AT1 also contribute to the inhibition of PMN apoptosis.

Spontaneous PMN apoptosis has been shown to be a caspase-dependent apoptotic program because PMNs incubated with caspase inhibitors do not undergo apoptosis and can be triggered by extrinsic and intrinsic apoptotic pathways (47). There are several studies that associate spontaneous PMN apoptosis with intrinsic mitochondrial signaling, including a decline in antiapoptotic protein Mcl-1, translocation of proapoptotic Bax to the mitochondrium, and subsequent release of cytochrome c and caspase 9 activation (48, 49). Other studies have described caspase 8–dependent spontaneous PMN apoptosis, involving ligand-independent clustering of death receptors (24). Caspases 8 and 9 can then activate effector caspase 3, which is critical for spontaneous and TNF-α–induced apoptosis pathways in PMNs (24, 25, 50, 51). Distinguishing between the intrinsic (caspase 9) and extrinsic (caspase 8) activation pathways is difficult because caspase 9 can also activate caspase 8, thereby intertwining these pathways. Thus, our observations that caspase 8 and 9 activities are inhibited by incubation of PMNs in RCoV-AT1 can suggest that the intrinsic pathway, whereby caspase 9 activation leads to caspase 8 activation, or both intrinsic and extrinsic pathways are involved. Our finding that RCoV-AT1 inhibits TNF-α–induced PMN apoptosis, but not UV irradiation– or Cx-induced PMN apoptosis, further supports inhibition of the caspase 8–dependent extrinsic pathway (47). Caspase 2, which can be activated by Fas-Associated protein with Death Domain–independent extrinsic pathways or intrinsic cellular stress pathways, was not inhibited by incubation of PMN in RCoV-AT1 medium. However, we evaluated caspase 2 activity through 4 hours of incubation. It is possible that RCoV-AT1 could inhibit caspase 2 activity at later time points. Although death domain–mediated activation of caspase 2 occurs very early, activation through stress-response pathways might occur later in the PMN

lifespan. The role of caspase 2 in PMN apoptosis has not been defined. Here, we show that caspase 2 activity increased upon incubation of rat PMNs *in vitro*. However, PMN apoptosis was inhibited by RCoV-AT1 medium despite activation of caspase 2. This suggests that caspase 2 activity is not sufficient to induce PMN apoptosis. This is in agreement with other studies that demonstrate that activation of caspase 2 in the absence of caspase 8 is not sufficient to mediate Fas-induced apoptosis in T cells (27).

Because alveolar epithelial cells are important targets for viral infection in the lung, a complete understanding of their contributions to inflammatory responses is needed. These studies defined the molecular mechanisms whereby virus-infected alveolar cells direct chemotaxis and inhibit spontaneous and induced PMN apoptosis. The relevance of these interactions during infection *in vivo* will further our understanding of viral pathogenesis in the lung. Rodent models of respiratory viral infections allow us to delineate molecular mechanisms in primary cells *in vitro* and correlate these findings with pathogenesis studies in the animal.

Author disclosures are available with the text of this article at www.atsjournals.org.

Acknowledgments: The authors thank Dr. Julian Leibowitz and Dr. Kathryn Holmes for reagents and Ms. Ann Norton and Dr. Keun Seok Seo for help with the flow cytometry.

References

1. Shieh W-J, Blau DM, Denison AM, DeLeon-Carnes M, Adem P, Bhatnagar J, Sumner J, Liu L, Patel M, Batten B, *et al*. 2009 Pandemic Influenza A (H1N1): pathology and pathogenesis of 100 fatal cases in the United States. *Am J Pathol* 2010;177:166–175.
2. Johnson JE, Gonzales RA, Olson SJ, Wright PF, Graham BS. The histopathology of fatal untreated human respiratory syncytial virus infection. *Mod Pathol* 2007;20:108–119.
3. Nicholls JM, Butany J, Poon LL, Chan KH, Beh SL, Poutanen S, Peiris JS, Wong M. Time course and cellular localization of SARS-CoV nucleoprotein and RNA in lungs from fatal cases of SARS. *PLoS Med* 2006; 3:e27.
4. Uiprasertkul M, Kitphati R, Puthavathana P, Kriwong R, Kongchanagul A, Ungchusak K, Angkasekwinai S, Chokephaibulkit K, Srisook K, Vanprapar N, *et al*. Apoptosis and pathogenesis of avian influenza a (H5N1) virus in humans. *Emerg Infect Dis* 2007;13:708–712.
5. Roberts A, Deming D, Paddock CD, Cheng A, Yount B, Vogel L, Herman BD, Sheahan T, Heise M, Genrich GL, *et al*. A mouse-adapted SARS-coronavirus causes disease and mortality in balb/c mice. *PLoS Pathog* 2007;3:e5.
6. Haagmans BL, Kuiken T, Martina BE, Fouchier RA, Rimmelzwaan GF, van Amerongen G, van Riel D, de Jong T, Itamura S, Chan KH, *et al*. Pegylated interferon-alpha protects type 1 pneumocytes against SARS coronavirus infection in macaques. *Nat Med* 2004;10:290–293.
7. Narasaraju T, Yang E, Samy RP, Ng HH, Poh WP, Liew AA, Phoon MC, van Rooijen N, Chow VT. Excessive neutrophils and neutrophil extracellular traps contribute to acute lung injury of influenza pneumonitis. *Am J Pathol* 2011;179:199–210.
8. Tate MD, Ioannidis LJ, Croker B, Brown LE, Brooks AG, Reading PC. The role of neutrophils during mild and severe influenza virus infections of mice. *PLoS ONE* 2011;6:e17618.
9. Shornick LP, Wells AG, Zhang Y, Patel AC, Huang G, Takami K, Sosa M, Shukla NA, Agapov E, Holtzman MJ. Airway epithelial versus immune cell stat1 function for innate defense against respiratory viral infection. *J Immunol* 2008;180:3319–3328.
10. Miura TA, Holmes KV. Host-pathogen interactions during coronavirus infection of primary alveolar epithelial cells. *J Leukoc Biol* 2009;86: 1145–1151.
11. Wang J, Edeen K, Manzer R, Chang Y, Wang S, Chen X, Funk CJ, Cosgrove GP, Fang X, Mason RJ. Differentiated human alveolar epithelial cells and reversibility of their phenotype in vitro. *Am J Respir Cell Mol Biol* 2007;36:661–668.
12. Qiao R, Zhou B, Liebler JM, Li X, Crandall ED, Borok Z. Identification of three genes of known function expressed by alveolar epithelial type I cells. *Am J Respir Cell Mol Biol* 2003;29:98–105.
13. Wang J, Nikrad MP, Phang T, Gao B, Alford T, Ito Y, Edeen K, Travanty EA, Kosmider B, Hartshorn K, *et al*. Innate immune response to influenza A virus in differentiated human alveolar type II cells. *Am J Respir Cell Mol Biol* 2011;45:582–591.
14. Yu WC, Chan RW, Wang J, Travanty EA, Nicholls JM, Peiris JS, Mason RJ, Chan MC. Viral replication and innate host responses in primary human alveolar epithelial cells and alveolar macrophages infected with influenza H5N1 and H1N1 viruses. *J Virol* 2011;85:6844–6855.
15. Funk CJ, Manzer R, Miura T, Groshong SD, Ito Y, Travanty E, Leete J, Holmes K, Mason RJ. Rat respiratory coronavirus infection: replication in airway and alveolar epithelial cells and innate immune response. *J Gen Virol* 2009;90:2956–2964.
16. Miura TA, Wang J, Holmes KV, Mason RJ. Rat coronaviruses infect rat alveolar type I epithelial cells and induce expression of CXC chemokines. *Virology* 2007;369:288–298.
17. Frevert CW, Wong VA, Goodman RB, Goodwin R, Martin TR. Rapid fluorescence-based measurement of neutrophil migration in vitro. *J Immunol Methods* 1998;213:41–52.
18. Shibata F, Konishi K, Nakagawa H. Identification of a common receptor for three types of rat cytokine-induced neutrophil chemoattractants (CINCs). *Cytokine* 2000;12:1368–1373.
19. Auten RL, Richardson RM, White JR, Mason SN, Vozzelli MA, Whorton MH. Nonpeptide CXCR2 antagonist prevents neutrophil accumulation in hyperoxia-exposed newborn rats. *J Pharmacol Exp Ther* 2001;299:90–95.
20. Nesmelova IV, Sham Y, Dudek AZ, van Eijk LI, Wu G, Slungaard A, Mortari F, Griffioen AW, Mayo KH. Platelet factor 4 and interleukin-8 CXC chemokine heterodimer formation modulates function at the quaternary structural level. *J Biol Chem* 2005;280:4948–4958.
21. Nasser MW, Raghuwanshi SK, Grant DJ, Jala VR, Rajarathnam K, Richardson RM. Differential activation and regulation of CXCR1 and CXCR2 by CXCL8 monomer and dimer. *J Immunol* 2009;183: 3425–3432.
22. Das ST, Rajagopalan L, Guerrero-Plata A, Sai J, Richmond A, Garofalo RP, Rajarathnam K. Monomeric and dimeric CXCL8 are both essential for in vivo neutrophil recruitment. *PLoS ONE* 2010;5:e11754.
23. Dunican A, Grutkoski P, Leuenroth S, Ayala A, Simms HH. Neutrophils regulate their own apoptosis via preservation of CXC receptors. *J Surg Res* 2000;90:32–38.
24. Scheel-Toellner D, Wang K, Craddock R, Webb PR, McGettrick HM, Assi LK, Parkes N, Clough LE, Gulbins E, Salmon M, *et al*. Reactive oxygen species limit neutrophil life span by activating death receptor signaling. *Blood* 2004;104:2557–2564.
25. Daigle I, Simon H-U. Critical role for caspases 3 and 8 in neutrophil but not eosinophil apoptosis. *Int Arch Allergy Immunol* 2001;126:147–156.
26. Lassus P, Opitz-Araya X, Lazebnik Y. Requirement for caspase-2 in stress-induced apoptosis before mitochondrial permeabilization. *Science* 2002;297:1352–1354.
27. Lavrik IN, Golks A, Baumann S, Krammer PH. Caspase-2 is activated at the CD95 death-inducing signaling complex in the course of CD95-induced apoptosis. *Blood* 2006;108:559–565.
28. Lindemans CA, Coffer PJ, Schellens IMM, de Graaff PMA, Kimpen JLL, Koenderman L. Respiratory syncytial virus inhibits granulocyte apoptosis through a phosphatidylinositol 3-kinase and NF-{kappa}B-dependent mechanism. *J Immunol* 2006;176:5529–5537.
29. Dunican AL, Leuenroth SJ, Ayala A, Simms HH. CXC chemokine suppression of polymorphonuclear leukocytes apoptosis and preservation of function is oxidative stress independent. *Shock* 2000;13:244–250.
30. Kettritz R, Gaido ML, Haller H, Luft FC, Jennette CJ, Falk RJ. Interleukin-8 delays spontaneous and tumor necrosis factor-[alpha]-mediated apoptosis of human neutrophils. *Kidney Int* 1998;53:84–91.
31. Dunstan CA, Salafranca MN, Adhikari S, Xia Y, Feng L, Harrison JK. Identification of two rat genes orthologous to the human interleukin-8 receptors. *J Biol Chem* 1996;271:32770–32776.
32. Shibata F, Konishi K, Kato H, Komorita N, al-Mokdad M, Fujioka M, Nakagawa H. Recombinant production and biological properties of rat cytokine-induced neutrophil chemoattractants, GRO/CINC-2 alpha, CINC-2 beta and CINC-3. *Eur J Biochem* 1995;231:306–311.

33. Chandrasekar B, Melby PC, Sarau HM, Raveendran M, Perla RP, Marelli-Berg FM, Dulin NO, Singh IS. Chemokine-cytokine cross-talk: the ELR+ CXC chemokine LIX (CXCL5) amplifies a proinflammatory cytokine response via a phosphatidylinositol 3-kinase-NF-kappa B pathway. *J Biol Chem* 2003;278:4675–4686.
34. Arnold R, Werner F, Humbert B, Werchau H, Konig W. Effect of respiratory syncytial virus-antibody complexes on cytokine (IL-8, IL-6, TNF-alpha) release and respiratory burst in human granulocytes. *Immunology* 1994;82:184–191.
35. Colotta F, Re F, Polentarutti N, Sozzani S, Mantovani A. Modulation of granulocyte survival and programmed cell death by cytokines and bacterial products. *Blood* 1992;80:2012–2020.
36. Colamussi ML, White MR, Crouch E, Hartshorn KL. Influenza A virus accelerates neutrophil apoptosis and markedly potentiates apoptotic effects of bacteria. *Blood* 1999;93:2395–2403.
37. Glynn PC, Henney E, Hall IP. The selective CXCR2 antagonist SB272844 blocks interleukin-8 and growth-related oncogene-[alpha]-mediated inhibition of spontaneous neutrophil apoptosis. *Pulm Pharmacol Ther* 2002;15:103–111.
38. Wang Y, Luo W, Stricker R, Reiser G. Protease-activated receptor-1 protects rat astrocytes from apoptotic cell death via JNK-mediated release of the chemokine GRO/CINC-1. *J Neurochem* 2006;98:1046–1060.
39. Girard D, Paquet ME, Paquin R, Beaulieu AD. Differential effects of interleukin-15 (IL-15) and IL-2 on human neutrophils: modulation of phagocytosis, cytoskeleton rearrangement, gene expression, and apoptosis by IL-15. *Blood* 1996;88:3176–3184.
40. Cox G, Gauldie J, Jordana M. Bronchial epithelial cell-derived cytokines (G-CSF and GM-CSF) promote the survival of peripheral blood neutrophils in vitro. *Am J Respir Cell Mol Biol* 1992;7:507–513.
41. Afford SC, Pongracz J, Stockley RA, Crocker J, Burnett D. The induction by human interleukin-6 of apoptosis in the promonocytic cell line U937 and human neutrophils. *J Biol Chem* 1992;267:21612–21616.
42. Tsuchida H, Takeda Y, Takei H, Shinzawa H, Takahashi T, Sendo F. In vivo regulation of rat neutrophil apoptosis occurring spontaneously or induced with TNF-alpha or cycloheximide. *J Immunol* 1995;154:2403–2412.
43. Takeda Y, Watanabe H, Yonehara S, Yamashita T, Salto S, Sendo F. Rapid acceleration of neutrophil apoptosis by tumor necrosis factor-{alpha}. *Int Immunol* 1993;5:691–694.
44. Biffl WL, Moore EE, Moore FA, Barnett CC. Interleukin-6 suppression of neutrophil apoptosis is neutrophil concentration dependent. *J Leukoc Biol* 1995;58:582–584.
45. van den Berg JM, Weyer S, Weening JJ, Roos D, Kuijpers TW. Divergent effects of tumor necrosis factor {alpha} on apoptosis of human neutrophils. *J Leukoc Biol* 2001;69:467–473.
46. Murray J, Barbara JAJ, Dunkley SA, Lopez AF, Van Ostade X, Condliffe AM, Dransfield I, Haslett C, Chilvers ER. Regulation of neutrophil apoptosis by tumor necrosis factor-alpha: requirement for TNFR55 and TNFR75 for induction of apoptosis in vitro. *Blood* 1997;90:2772–2783.
47. Maianski NA, Roos D, Kuijpers TW. Tumor necrosis factor alpha induces a caspase-independent death pathway in human neutrophils. *Blood* 2003;101:1987–1995.
48. Fossati G, Moulding DA, Spiller DG, Moots RJ, White MR, Edwards SW. The mitochondrial network of human neutrophils: role in chemotaxis, phagocytosis, respiratory burst activation, and commitment to apoptosis. *J Immunol* 2003;170:1964–1972.
49. Moulding DA, Quayle JA, Hart CA, Edwards SW. Mcl-1 expression in human neutrophils: regulation by cytokines and correlation with cell survival. *Blood* 1998;92:2495–2502.
50. Kettritz R, Xu Y-X, Faass B, Klein JB, Muller E-C, Otto A, Busjahn A, Luft FC, Haller H. TNF-{alpha}-mediated neutrophil apoptosis involves LY-GDI, a RHO GTPase regulator. *J Leukoc Biol* 2000;68:277–283.
51. Pongracz J, Webb P, Wang K, Deacon E, Lunn OJ, Lord JM. Spontaneous neutrophil apoptosis involves caspase 3-mediated activation of protein kinase C-delta. *J Biol Chem* 1999;274:37329–37334.